Ecosystems
DOI: 10.1007/s10021-014-9758-4

ECOSYSTEMS


# Gross Primary Productivity of a High Elevation Tropical Montane Cloud Forest

Martine Janet van de Weg,[1,2]* Patrick Meir,[2,3] Mat Williams,[4] Cécile Girardin,[5] Yadvinder Malhi,[5] Javier Silva-Espejo,[6] and John Grace[3]

[1]*Amsterdam Global Change Institute, Vrije Universiteit Amsterdam, De Boelenlaan 1085, 1081 HV Amsterdam, The Netherlands;* [2]*School of Geosciences, University of Edinburgh, Drummond Street, Edinburgh EH8 9XP, UK;* [3]*Research School of Biology, Australian National University, Canberra, ACT 0200, Australia;* [4]*School of Geosciences, University of Edinburgh, Crew Building, Edinburgh EH9 3JNB, UK;* [5]*Environmental Change Institute, School of Geography and the Environment, University of Oxford, South Parks Road, Oxford OX1 3QY, UK;* [6]*Universidad San Antonio Abad del Cusco, Avenida de la Cultura No 73, Cuzco, Peru*

## Abstract

For decades, the productivity of tropical montane cloud forests (TMCF) has been assumed to be lower than in tropical lowland forests due to nutrient limitation, lower temperatures, and frequent cloud immersion, although actual estimates of gross primary productivity (GPP) are very scarce. Here, we present the results of a process-based modeling estimate of GPP, using a soil–plant–atmosphere model, of a high elevation Peruvian TMCF. The model was parameterized with field-measured physiological and structural vegetation variables, and driven with meteorological data from the site. Modeled transpiration corroborated well with measured sap flow, and simulated GPP added up to 16.2 ± SE 1.6 Mg C $ha^{-1}$ $y^{-1}$. Dry season GPP was significantly lower than wet season GPP, although this difference was 17% and not caused by drought stress. The strongest environmental controls on simulated GPP were variation of photosynthetic active radiation and air temperature ($T_{air}$). Their relative importance likely varies with elevation and the local prevalence of cloud cover. Photosynthetic parameters ($V_{cmax}$ and $J_{max}$) and leaf area index were the most important non-environmental controls on GPP. We additionally compared the modeled results with a recent estimate of GPP of the same Peruvian TMCF derived by the summing of ecosystem respiration and net productivity terms, which added up to 26 Mg C $ha^{-1}$ $y^{-1}$. Despite the uncertainties in modeling GPP we conclude that at this altitude GPP is, conservatively estimated, 30–40% lower than in lowland rainforest and this difference is driven mostly by cooler temperatures than changes in other parameters.

**Key words:** SPA model; sap flow; diurnal photosynthesis; carbon fluxes; Peru; Andes; gross primary productivity (GPP); net primary productivity (NPP); autotrophic respiration; carbon expenditure.

## Introduction

Characterized by the frequent occurrence of clouds and mist and usually found between 1,000 and 3,000 m above sea level (a.s.l.), tropical montane cloud forests (TMCF) differ from lowland rainforests in both their structure and functioning. For example, the TMCF tree stature is smaller, their

Received 9 October 2013; accepted 30 January 2014

**Electronic supplementary material:** The online version of this article (doi:10.1007/s10021-014-9758-4) contains supplementary material, which is available to authorized users.

**Author's Contribution:** PM, JG, and MvdW conceived of the study, MvdW, CG, and JS-E conducted the fieldwork, MvdW and CG analyzed the field work data, JS-E and YM provided additional field data, MW contributed the model, MvdW analyzed the model outcomes and all authors contributed to the manuscript.

**Corresponding author; e-mail:* m.j.vande.weg@vu.nl

Published online: 08 March 2014

leaves have a higher leaf mass per area (LMA), and leaf area index (LAI) is lower (for example, Grubb and Whitmore 1966; Tanner and others 1998; Kitayama and Aiba 2002; Moser and others 2007; van de Weg and others 2009). TMCFs net primary productivity (NPP) is also low compared with lowland rainforests, and productivity decreases with increasing altitude in rates ranging between 1.0 and 6.6 Mg C $ha^{-1}$ $y^{-1}$ $km^{-1}$ (Raich and others 1997; Kitayama and Aiba 2002; Girardin and others 2010). Explanations for the lower productivity of TMCFs include the lower levels of photosynthetic active radiation (PAR) because of frequent cloud immersion, lower average temperatures, periodic water deficiencies, leaf wetness that potentially inhibits photosynthesis, and lower nutrient supply (Bruijnzeel and Veneklaas 1998; Waide and others 1998; Letts and Mulligan 2005). The latter hypothesis has been tested by adding nutrients (nitrogen and phosphorus) to this ecosystem and in some cases, but not all, this resulted in increased TMCF stem growth and litter fall (for example, Tanner and others 1990, 1992; Vitousek and Farrington 1997; Adamek and others 2009; Fisher and others 2013). However, the influence of environmental variables, such as the lower total incident PAR and lower temperatures, has not been tested experimentally, or through detailed process-based modeling. Nonetheless, both light and temperature have been regarded to be key environmental controls on TMCF productivity (Bruijnzeel and Veneklaas 1998).

Overall, estimates of TMCF gross primary productivity (GPP) are rare, probably also because observations of stand-scale $CO_2$ fluxes with the eddy covariance technique are difficult in the mountainous terrains of TMCFs (Kaimal and Finnigan 1994). However, contrasting with the paradigm of decreasing productivity with increasing altitude, a recent calculation of the GPP of an Andean TMCF at 3,025 m a.s.l. resulted in estimates of 25.9 ± 3.1 Mg C $ha^{-1}$ $y^{-1}$ (Girardin and others 2013). This GPP value is only slightly lower than observed values from tropical lowland Amazonian rainforests (for example, Fisher and others 2007; Hutyra and others 2008; Malhi and others 2009; Miller and others 2004), which range from 30 to 40 Mg C $ha^{-1}$ $y^{-1}$. The GPP estimate of 25.9 Mg C $ha^{-1}$ $y^{-1}$ was based on quantifying the carbon expenditure of the forest, summing all the autotrophic respiration ($R_a$) and NPP components of the ecosystem (for example, Ryan and others 2004). Other TMCF GPP estimates are based on modeling exercises, although these studies are also scarce. Wang and others (2003) modeled annual GPP values of 60.32–24.08 Mg C $ha^{-1}$ $y^{-1}$ over an altitudinal range of 450–1,050 m a.s.l., respectively, in the Luquillo mountains in Puerto Rico, using a canopy process model driven with simulated climate data from a topographical climate model and remotely sensed LAI data derived from NDVI measurements. However, for the high altitude sites this model overestimated GPP up to 40% compared with field observations. In addition, (Marthews and others 2012) modeled the GPP of a Peruvian TMCF with the land surface model JULES, but their simulation returned values of only 1.25 Mg C $ha^{-1}$ $y^{-1}$, which was the result of the model not capturing TMCF vegetation very well. In sum, there are still very few estimates of GPP in TMCFs, and consequently, questions regarding the environmental controls on GPP in TMCFs remain open.

In this study, we simulated the GPP of a TMCF at 3,025 m a.s.l. in Peru with the process-based soil–plant–atmosphere (SPA) model developed by (Williams and others 1996, 2001a). The SPA model has performed well in simulating a wide range of ecosystems (Williams and others 1996, 2001a, b; Wright and others 2013) and simulated the C and $H_2O$ fluxes of an Amazonian lowland rainforest particularly well when the model output was evaluated against stomatal conductance, sap flow and eddy covariance measurements (Fisher and others 2006, 2007, 2008; Williams and others 1998). For our study, we parameterized the model with data collected by ourselves and others, from the same site investigated by (Girardin and others 2013). We used in situ measured leaf photosynthetic parameters and leaf traits, canopy, root and soil structure data, and the model was driven with a year of weather data recorded at the same site. Validation of the model's performance was done by comparing it with in situ collected sap flow data, and simulated leaf-level photosynthesis of the upper canopy layer with some in situ measurements. We investigated how TMCF GPP is controlled by environmental conditions and canopy structure, as informed by analyses of SPA (Fisher and others 2007; Fox and others 2009). The hypotheses we tested were: (1) TMCF GPP is lower than observed in tropical lowland forests. (2) The key environmental determinants of lower TMCF GPP are temperature and PAR, whereas water deficiencies are of little importance under the current climate. (3) GPP varies little throughout the seasons, as temperature and PAR are expected not to change substantially throughout the season. In addition, we discuss the discrepancies between our process-based modeled results and the GPP esti-

mates of (Girardin and others 2013) made by summing growth and autotrophic respiration terms.

## Methods

### Research Site

The TMCF that we simulated with the SPA model is a 1-ha plot in the Kosñipata valley in Peru at 3,025 m a.s.l. (13°11′28″S/71°35′24″W). The plot is located in the cultural buffer zone of the Parque Nacional del Manú, Cusco, near the Wayquecha Research Station. The vegetation is a closed canopy forest with a relatively low mean canopy height 12.8 ± SE 0.46 m ($n$ = 180), with average soil depth of 0.44 ± SE 0.06 m ($n$ = 20). Average annual air temperature ($T_{air}$) is 12.5°C, and annual rainfall ranges between 1,700 and 2,000 mm $y^{-1}$. The forest is dominated by species in the *Weinmannia* and *Clusia* genera that together represent 56% of the number of trees in the plot, with *Weinmannia crassifolia* being the most dominant of species (~35% of individual trees).

### Meteorology

An automated weather station (Campbell Scientific Ltd, UK) collected and stored meteorological data using a data logger (CR3000, Campbell Scientific Ltd, UK). Precipitation was measured with a tipping bucket rainfall gauge, together with two fog collectors (harp and mesh), all three with a 0.2 mm resolution (Campbell Scientific Ltd, UK). PAR was measured with a PAR quantum sensor (Skye Instruments Ltd, Powys, UK), whereas a net radiometer measured short-wave radiation (SWR) (CNR1, Kipp & Zonen, Delft, Netherlands) and the diffuse radiation was registered with a sunshine sensor (BF3, Delta-T Devices Ltd, Cambridge, UK). $T_{air}$ and relative humidity were measured with a combined HMT sensor (Vaisala, Oy, Finland), and vapor pressure deficit (VPD) was automatically calculated from those data. Wind speed measurements failed for this period, except for 9 days, so average wind speed in the model was set at 1.0 m $s^{-1}$. Other meteorological data were missing from 27 February 2009 to 3 March 2009 and for 30 April 2009. Data for these two gaps were filled with mean monthly diurnal values. For SWR, data were missing from 19 September 2008 to 9 December 2008, representing 22% of the SWR dataset. These gaps were filled by recalculating the SWR from the collected PAR data in that period, using a regression from the available PAR and SWR data.

### Sap Flux

To validate the results of the SPA model we used sap flow rates, measured on 12 trees in the research plot. The species included were *Clusia cretosa* (Hammel ined.) (five trees), *W. crassifolia* (three trees), *Prunus integrifolia* (one tree), *Clusia flavifora* (one tree), *Weinmannia bangii* (one tree), and a *Clethra* species not identified to species level (one tree). Sap flow sensors were installed in April–May 2007 on trees that represented the diameter at breast height (DBH) distribution present in the plot (12.9–38.1 cm). Measurements were made using the trunk segment heat balance method described by Čermák and others (1973, 2004) (Sap Flux Meter P4.1, Environmental Measuring Systems, Brno, Czech Republic). Limited power supply throughout the year restricted the data collection period between 16 July 2008 and 1 September 2008, with 5 days missing because of power failure. Because the sap flow rates per sapwood area ($J$, g $m^{-2}$ $s^{-1}$) were proportional to the basal areas of the measured trees, plot level sap flow could consequently be scaled with the plot basal area.

### Photosynthesis and Water Potential Measurements

The Rubisco carboxylation efficiency ($V_{cmax}$) and electron transport efficiency ($J_{max}$), which are the photosynthetic parameters needed for the model, were derived from $A$–$C_i$ curves measured on *W. crassifolia*, *Clethra cuneata*, *Schefflera allocotantha*, *P. integrifolia*, and *C. cretosa*. We used portable photosynthesis equipment fitted with an LED light source (a Li-Cor 6400 with a 6400-02B Red/Blue Light Source, Li-Cor, Lincoln Inc.) and the $A$–$C_i$ curves were performed at an average temperature of 20.4°C (±SE 0.3°C) because observed in situ mid-day leaf temperatures ranged between 15 and 25°C. A detailed description of the $A$–$C_i$ curves and curve-fitting routine is found in Supplementary Information I and in (van de Weg and others 2012). The average $V_{cmax}$ and $J_{max}$ per canopy layer in the model were consequently based on the (proportional) basal area per species and their estimated presence per canopy layer (Table 1, Supplementary Information I).

To validate the modeled foliar photosynthesis rates ($A_{net}$) and the leaf temperatures ($T_{leaf}$), in situ data for $A_{net}$ and $T_{leaf}$ were collected on individuals next to the research plot and that were fully sunlit and accessible from the ground to guarantee an intact water column. For $A_{net}$, fully sunlit, non-damaged leaves of *W. crassifolia*, *C. cuneata*,

**Table 1.** Photosynthetic Parameters $V_{cmax}$ and $J_{max}$ per Canopy Layer and Proportion of Leaves per Canopy Layer as Represented in a Standard Run of the SPA Model

| Canopy layer (1 = top canopy) | $V_{cmax}$ (μmol $m^{-2}$ $s^{-1}$) | $J_{max}$ (μmol $m^{-2}$ $s^{-1}$) | Proportion of leaves per layer |
|---|---|---|---|
| 1 | 45.9 | 95.2 | 0.203 |
| 2 | 34.6 | 81.2 | 0.350 |
| 3 | 28.3 | 62.5 | 0.214 |
| 4 | 23.2 | 50.9 | 0.143 |
| 6 | 12.8 | 29.1 | 0.052 |
| 7 | 15.4 | 30.6 | 0.017 |
| 8 | 15.1 | 29.9 | 0.011 |
| 9 | 0 | 0 | 0 |
| 10 | 0 | 0 | 0 |

*S. allocotantha*, and *C. cretosa* were measured on 14, 24, and 28 August 2008 between 06:00 and 17:00 on one or two leaves from three individual trees per species. The light source of the Li-Cor 6400 was set in the mode to follow the ambient PAR observed by the external quantum sensor of the Li-Cor 6400 head. This setting was preferred over using the leaf chamber with a transparent top, to avoid shading of the 6 $cm^2$ leaf area in the cuvette, caused by the cuvette frame under certain angels of ambient illumination. $T_{leaf}$ measurements were derived from these photosynthesis measurements and from a dataset collected with a portable dynamic diffusion porometer (Delta-T AP4, Delta-T Devices Ltd, Cambridge, UK), which is equipped with a leaf-contact thermocouple. In total, $T_{leaf}$ was measured on five individuals for the same species on three sunlit leaves between 6:00 and 17:00 on 19, 21, 23, and 28 July and 14, 24, and 28 August 2008.

On the same days as the $T_{leaf}$ measurements, minimum leaf water potential ($\Psi_{leaf}$) was measured with a pressure chamber (Skye Instruments Ltd, Powys, UK) on the same four species to obtain the minimum $\Psi_{leaf}$ to parameterize the SPA model with.

## Structural Vegetation and Soil Characteristics

The gap fraction of the canopy was determined using a hand-held spherical densiometer (Lemmon 1956). We derived the LAI in July 2008 at 180 locations equally distributed in the 1 ha research plot, to get a large spatial coverage plot LAI. Average dry season LAI was similar to dry season values from Girardin and others (2013), being 4.2 ± 0.04 and 4.1 ± 0.15, respectively. Monthly changes in LAI throughout the year were then based on the variability provided by Girardin and others (2013), who used the hemispherical photographic method on 25 locations in the research plot. The fraction LAI per canopy layer (top-middle-canopy) was estimated visually from the trees from which $V_{cmax}$ and $J_{max}$ values had been measured ($n$ = 25). Root biomass, root density, and root biomass density values were taken from Girardin and others (2010) and rooting depth of fine roots was up to 30 cm. Soil properties (organic fraction, sand and clay fraction of the soil) were adapted from (Zimmermann and others 2009) and soil porosity was calculated according to (Saxton and others 1986).

## Modeling Methodology

A detailed description of the SPA model (v. 1) is found in (Williams and others 1996, 2001a). The model runs at 30-min time steps and explicitly simulates the radiative transfer of direct and diffuse PAR through ten separate canopy layers. Foliar C-uptake is based on the Farquhar equation for $C_3$ photosynthesis (Farquhar and others 1980) and the Penman–Monteith equation determines leaf-level transpiration. These two processes are linked by a model of stomatal conductance that optimizes daily C gain, while maintaining $\Psi_{leaf}$ above the threshold value. Maximum stomatal conductance ($g_s$) was set at 0.5 mol $m^{-2}$ $s^{-1}$, which approximates maximum observed $g_s$. Iota ($\iota$, dimensionless), the parameter that determines the minimal increase in photosynthesis necessary for stomata to open, was set at 1.0007 (that is, $g_s$ is incremented until C-uptake no longer increases by more than $1 - \iota$, as long as minimum $\Psi_{leaf}$ is not crossed). Furthermore, the temperature response curves of the photosynthetic parameters $V_{cmax}$ and $J_{max}$ are fitted to the polynomial relationships found in (McMurtrie and others 1992).

The SPA model also couples canopy transpiration with hydraulic transport from the root system,

**Table 2.** Structural Parameters and Their Units Used in the Standard SPA Model Simulations and Their Origins

| Parameter | Units | Value | Source |
|---|---|---|---|
| Canopy height | m | 12.8 | Field observations |
| Aboveground conductance | $m^2$ MPa $mmol^{-1}$ | 3.5 | Parameterised according to leaf-specific conductivity (LSC) |
| Root resistivity | MPa s g $mmol^{-1}$ | 140 | Parameterised according to LSC |
| Rooting depth | m | 0.3 | Field observations |
| Iota | dimensionless | 0.0007 | Set |
| Capacitance | mmol $MPa^{-1}$ $m^{-2}$ | 5,000 | Set |

simulating hourly and daily sap flow directly. The inclusion of a capacitance term in the hydraulic model generates a time lag between leaf losses and stem transport of water, and was set to 5,000 mmol $MPa^{-1}$ $m^{-2}$, which matched the tails of in situ hourly sap flow during each evening. The hydraulic conductivities (that is, stem conductivity and root resistivity) were calibrated with leaf-specific conductance (LSC, mmol $m^{-2}$ $s^{-1}$ $MPa^{-1}$), assuming aboveground and belowground hydraulic resistance to be approximately equal (Table 2). LSC was calculated with independent transpiration measurements ($E$, mmol $m^{-2}$ $s^{-1}$) and $\Psi_{leaf}$ measurements made from 2 to 5 August 2008 on four species that were selected for $A_{net}$ measurements, assuming:

$$\Delta\Psi = \Psi_{leaf} - \Psi_{predawn}$$

and

$$LSC = E/\Delta\Psi.$$

A detailed list of the model parameters and how they were retrieved can be found in Supplementary Information II.

## Sensitivity Analyses

Sensitivity analyses were performed for most of the model's parameters and environmental drivers to investigate which are the most important factors that control GPP in the SPA-simulated TMCF, given their range of observed values in the field (Table 3). In addition to providing absolute changes in GPP per changed parameter (ΔGPP), we determined their relative importance by dividing the proportional increase in parameter from minimum to maximum by the proportional increase or decrease in simulated GPP. Each factor was changed individually, keeping daily and seasonal variation proportional to the original observed values, while also keeping other drivers and parameters as in the original simulation. The sensitivity analyses for changes in $V_{cmax}$ and $J_{max}$ were conducted simultaneously because they vary in proportion with each other (Wullschleger 1993; Meir and others 2002). This simultaneous variation was also done for changes in PAR and SWR. Field measurements of capacitance and $\iota$ were not available, so we tested the sensitivity to changes of capacitance between 3,000 and 7,000 $MPa^{-1}$ $m^{-2}$, and for $\iota$ between 0.001 and 0.0001.

In addition, with three factors from the sensitivity test that explained a large part of the variation in the TMCF GPP ($T_{air}$, PAR and LAI), additional simulations were performed to estimate TMCF GPP under tropical lowland forests conditions. Again, temporal variation in the environmental drivers and LAI was kept proportional to the original observed values. The maximum values for the drivers $T_{air}$ and PAR, and the structural parameter LAI, did not originate from one particular tropical lowland site, but were set to rounded values within the range of values obtained from the literature (for example, Domingues and others 2005; Fisher and others 2007; Malhi and others 2009) (Table 4).

# Results

## Meteorology and Environmental Drivers

Precipitation was the strongest seasonal pattern in the meteorological drivers (Figure 1). The warmest month coincided with the wettest period, in November 2008 (11.2°C ± 1.1SD), whereas the coldest month was in the ''dry'' season in June 2009 (9.9°C ± 1.0SD). April 2009 had the lowest mean average PAR (based on 24 h averages) (18 mol $m^{-2}$ $day^{-1}$ ± 8SD) and September 2008 the highest (25 mol $m^{-2}$ $day^{-1}$ ± 17SD) (Figure 1B). Maximum daily VPD did not exceed 1.31 kPa, whereas the average daily VPD was

**Table 3.** Units and Standard Values for the Average Parameters Used in the SPA Model, and their Maximum and Minimum Values as Measured in the Field and Used in the Sensitivity Analyses

| Factor | Unit | Standard | Maximum | Minimum | ΔGPP (Mg C $ha^{-1}$ $y^{-1}$) | Ratio of change |
|---|---|---|---|---|---|---|
| Daily PAR | mol $m^{-2}$ $day^{-1}$ | 20.1 | 43.2 | 4.0 | 14.7 | 0.24 |
| $V_{cmax}/J_{max}$ | μmol $m^{-2}$ $s^{-1}$ | 46/95 | 93.9/140 | 14.9/26 | 14.3 | 0.46 |
| Daily SWR | MJ $m^{-2}$ $day^{-1}$ | 8.765 | 20.3 | 1.76 | 12.7 | 0.22 |
| LAI (N in leaves stays constant) | $m^{-2}$ $m^{-2}$ | 4.17 | 5.6 | 2.6 | 6.7 | 0.59 |
| Daily temperature | °C | 10.44 | 13.26 | 7.34 | 3.8 | 0.35 |
| Fraction diffuse light | – | 0.42 | 1 | 0.2 | 2.8 | 0.09 |
| LAI (N in canopy constant) | $m^{-2}$ $m^{-2}$ | 4.17 | 5.6 | 2.6 | 0.42 | 0.03 |
| Daily VPD | kPa | 0.14 | 0.36 | 0.03 | −0.05 | −0.01 |
| Total root biomass $m^{-2}$ | g | 3,291 | 5,420 | 1,967 | – | – |
| Root resistivity | MPa s g $mmol^{-1}$ | 145 | 180 | 120 | – | – |
| Plant conductivity | mmol $m^{-1}$ $s^{-1}$ $MPa^{-1}$ | 3.5 | 4.4 | 2.75 | – | – |
| Soil water content | $m^{-3}$ $m^{-3}$ | 0.29 | 0.367 | 0.196 | – | – |
| Iota ($\iota$) | dimensionless | 0.0007 | 0.001 | 0.0001 | – | – |
| Capacitance | mmol $m^{-2}$ LA $MPa^{-1}$ | 5,000 | 3,000 | 7,000 | – | – |

*The parameters are listed from top to bottom of which ΔGPP, the absolute change in GPP between model runs with minimum and maximum parameter values, was highest. Relative sensitivity per parameter of driver was calculated by dividing the % change in parameter or driver from minimum to maximum observed by the % change in simulated GPP. When ΔGPP was 0, no value for the ratio of change could be calculated.*

**Table 4.** The Factors Used to Simulate TMCF Under Typical Lowlands Tropical Rainforests Conditions, as well as the Simulated GPP and % in Increase Compared to a Standard Run of the SPA Model

| Factor | Unit | Value | Simulated GPP (Mg C $ha^{-1}$ $y^{-1}$) | % increase in GPP |
|---|---|---|---|---|
| $T_{air}$ | °C | 26 | 21.2 ± 2.1 | 30.3 |
| LAI | $m^{-2}$ $m^{-2}$ | 5.5 | 19.0 ± 1.9 | 17.2 |
| PAR | mol $m^{-2}$ $day^{-1}$ | 24.2 | 18.6 ± 1.9 | 14.9 |
| $T_{air}$ + PAR + LAI | | All above | 28.3 ± 2.8 | 74.9 |

*GPP = 16.24 Mg C $ha^{-1}$ $y^{-1}$.*

0.52 kPa. Even throughout the dry months May–September (average VPD was 0.21 kPa) days with very low VPD values (<0.007 kPa) occurred (Figure 1C).

## Modeled Sap Flux and Modeled GPP

The model simulated the hourly sap flow well, both for the values [$R^2$ = 0.87, root mean square error of approximation (RMSE) = 0.021 mm $h^{-1}$] and for the diurnal patterns (Figure 2). Daily sap flow is somewhat underestimated by the model (Figure 2A), but there was no systematic bias for days with either large or small transpiration values. Modeled transpiration was 223 mm $y^{-1}$ and total estimated annual GPP at 16.2 Mg C $ha^{-1}$ $y^{-1}$ (Figure 3A). Daily transpiration varied between 0.03 and 2.0 mm $day^{-1}$, whereas GPP varied from 1.91 to 6.87 g C $m^{-2}$ $day^{-1}$. Total transpiration and GPP varied throughout the year (Figure 3A), with daily GPP being significantly lower ($P < 0.001$, Student's $t$ test) in the dry season month June (39.9 kg C $ha^{-1}$ $day^{-1}$) compared with wet season month October (47.9 kg C $ha^{-1}$ $day^{-1}$). For these months, PAR and $T_{air}$ were significantly different as well, with daily PAR being 18 mol $m^{-2}$ $day^{-1}$ versus 23 mol $m^{-2}$ $day^{-1}$ ($P < 0.002$) and $T_{air}$ 9.9°C versus 10.7°C ($P < 0.002$), for June and October, respectively. Modeled transpiration was the lowest in December (0.37 ± 0.08 mm $day^{-1}$) when average VPD also had the lowest value (0.33 ± 0.04) kPa.

## Modeled and Measured Leaf-Level Photosynthesis and Leaf Temperature

The $A_{net}$ and $T_{leaf}$ measurements were not done continuously and not for all species on the same days, hindering a 1:1 comparison with the canopy-scale modeled output. Almost all the day-time

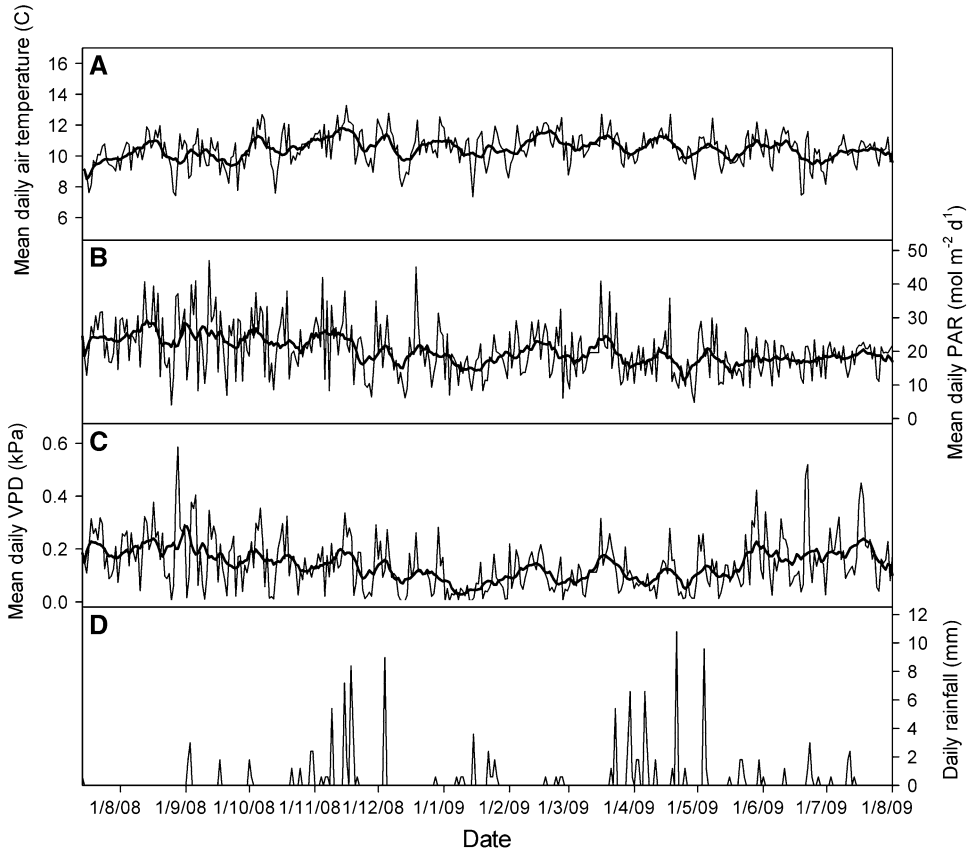


**Figure 1.** Meteorological variables as measured at the research site and used for driving the standard run of the SPA model for the period between 14 July 2008 and 13 July 2009 and their 10 daily average values (*thick line*). **A** Mean daily temperature, **B** mean daily photosynthetically active radiation (PAR), **C** mean daily VPD, and **D** total daily rainfall.

measured in situ $T_{leaf}$ values between 8:00 and 17:00 were higher than the modeled average $T_{leaf}$, from the upper canopy layer (layer 1 out of 10) (on average 3.25°C higher). Similarly, modeled maximum $A_{net}$ of the fully sunlit leaves from the top canopy layer was lower than for some of the in situ $A_{net}$ measurements, especially for *S. allocotantha* and *C. cuneata* (Figure 4C, D), although average modeled $A_{net}$ resembles the $A_{net}$ pattern from *W. crassifolia* leaves (Figure 4C, D).

## Sensitivity Analyses

In absolute terms, using the range in daily observed PAR values caused the largest ΔGPP (Table 3; Figure 5C), increasing GPP with 14.7 Mg C $ha^{-1}$ $y^{-1}$. However, if we look at what environmental parameter caused the largest relative change in GPP per relative parameter change, GPP was more sensitive to daily temperature (Table 3). Similarly for the vegetation parameters, absolute GPP values were most sensitive to changes in $V_{cmax}$ and $J_{max}$ (Table 3; Figure 5A). For relative sensitivity, however, LAI (with N in leaves staying constant) was the most important structural parameter (Table 3; Figure 5B). In contrast, GPP was insensitive to changes in environmental drivers or model parameters that were involved in the site's hydrology. For example, GPP was insensitive to changes in the range of observed mean daily VPD (Table 3; Figure 5D) and no effects on simulated GPP were found when changing capacitance, $\iota$, root biomass, and aboveground or belowground resistivity (Table 3). In fact, if we wanted to reduce simulated GPP by 1% through changes in plant resistivity, plant hydraulic conductance needed to be reduced to 0.2 mmol $m^{-1}$ $s^{-1}$ $MPa^{-1}$, which is a reduction of more than 90% from the minimum observed in the field (Table 3). Likewise, SWC had to be decreased to 0.1 (a value not observed in the dataset), to simulate any reduction in GPP.

Finally, changing some drivers and parameters to values found in lowland tropical forests showed that increasing $T_{air}$ increased modeled TMCF GPP by around 30% (Table 4). Increasing the PAR and LAI values increased GPP too, though less substantially (by 17 and 15%, respectively), while increasing all three factors simultaneously increased GPP by almost 75%.

# Discussion

## Simulating Transpiration

On a daily basis, modeled sap flow was a little lower though than observed daily sap flow, but for daily

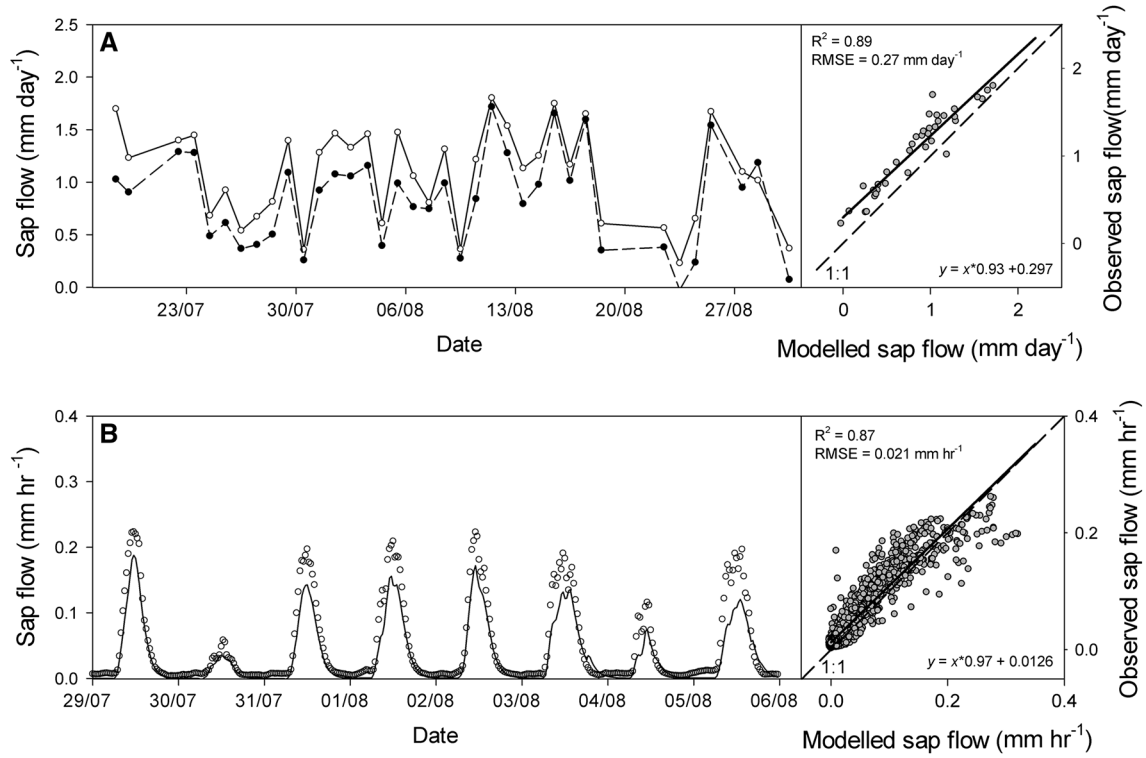


**Figure 2.** **A** Simulated (*black circles*) and observed (*open circles*) stand-scale daily sap flow for the period from 18 July 2008 to 31 August 2008. **B** Hourly sap flow (*open circles*) together with the modeled values (*line*) during one representative week from the period displayed in graph **A**. Both right panes show the modeled and observed sap flow values for the whole period July 2008 to 31 August 2008. *Dotted lines* represent 1:1 lines.

sap fluxes the modeled values were consistent in their onset, peak and ending compared to the observed patterns (Figure 2). This consistency with independent stomatal behavior data was also observed by earlier uses of the SPA model in tropical forests (for example, Fisher and others 2006, 2007). This suggests that the model simulates diurnal stomatal activity sufficiently well to simulate stand-scale water use within the range of meteorological drivers measured at our site. Our modeled transpiration rate of 223 mm $y^{-1}$ is slightly lower than the estimate of 250–300 mm from Bruijnzeel and Veneklaas (1998) but, consistent with these authors, much lower than values reported for tropical lowland rain forests (1,000–2,000 mm, Fisher and others 2009). Furthermore, simulated daily transpiration (up to 2.05 mm $day^{-1}$, average of 0.61 mm $day^{-1}$, Figure 3B) was comparable with ranges reported for TMCFs in Hawaii and Panama (0.39–1.02 mm $day^{-1}$, Zotz and others 1998; Santiago and others 2000), and similar to these forests, our sap flow measurements do not show mid-day stomatal closure (Figure 2B). The low TMCF transpiration rates are likely attributed to the low VPD values (that is, low atmospheric demand). Together with the insensitivity in transpiration at this site to changes in plant or soil hydraulic parameters and drivers (for example, root resistivity, plant conductance, Table 2) our analysis implies that a negative water balance in this forest is an unlikely scenario under current climatic conditions.

## Simulating GPP

In contrast with the transpiration, validating modeled GPP at high-temporal resolution is difficult because GPP can only be calculated when eddy covariance data are available, which they are not for this environment. At first sight, our GPP estimate of 16.2 Mg C $ha^{-1}$ $y^{-1}$ fits with the paradigm that GPP in TMCF is substantially lower than that of lowland tropical rain forests, because GPP values for the latter ecosystems vary between 30 and 40 Mg C $ha^{-1}$ $y^{-1}$ for Amazonian and Asian rainforests (for example, Hutyra and others 2008; Malhi and others 2009; Hirata and others 2008). If we assume that the SPA model captures the

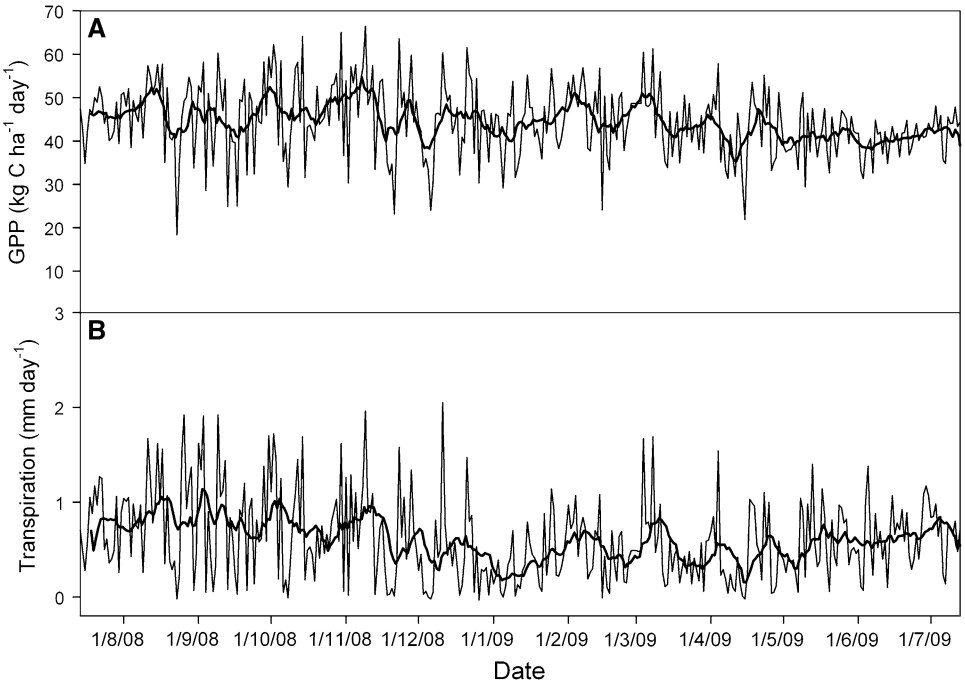


**Figure 3.** Simulated daily GPP (**A**) and transpiration (**B**), resulting from the standard input in the SPA model from 14 July 2008 to 13 July 2009. The *thick lines* represent a plot of data averaged as a 10-day running mean.

C-fluxes as well as the $H_2O$ fluxes, the modeled GPP supports our hypothesis (H1) that TMCF GPP is lower than the GPP of tropical lowland forests. Furthermore, extending the sensitivity analysis to represent a lowland–upland climate contrast, the increased ranges in $T_{air}$ and PAR associated with this contrast (Table 4) support the second hypothesis (H2) that $T_{air}$ is the most important factor controlling TMCF GPP over this elevation difference (~3,000 m). PAR is the second most important environmental control over this elevation difference, although it was most important in absolute terms for determining the natural variation in GPP at our site (Figure 5C). For a long time, both lower temperatures and PAR levels have been hypothesized to be important in limiting TMCF growth (Bruijnzeel and Veneklaas 1998; Waide and others 1998). Our analysis quantifies the relationship rigorously and enables an interpretation of their absolute and relative importance at the researched altitude. Changes in soil water content or VPD within the range of observed values were of little importance under the current climate in the 3,025 m a.s.l. TMCF, as they did not constrain modeled canopy gas exchange. The 17% difference in modeled GPP between the wet and dry season months October and June was a significant difference, contrary to what we hypothesized (H3). This difference is unlikely to be caused by actual drought stress (despite the term ''dry season''), given the insensitivity of the modeled forest to changes in the hydrological drivers and parameters (Table 3). It is most probably that the lower daily PAR and daily $T_{air}$ in June versus October (18 mol vs 23 mol $m^{-2}$ $day^{-1}$, and 9.9 versus 10.7°C, respectively) caused this difference.

For the structural and biochemical parameters of the model, GPP was most sensitive to changing the photosynthetic parameters $V_{cmax}$ and $J_{max}$, and LAI (Figure 4A, C), and insensitive to changes in the belowground structural parameters (Table 3). The latter might be because the simulated TMCF did not experience any high VPD values (as also supported by the sap flow data). The sensitivity of GPP to increases in $V_{cmax}$ and $J_{max}$ or LAI is consistent with the hypothesis that TMCF productivity is N-limited (Tanner and others 1998) if it is assumed that higher N availability would lead to more N investment in more leaves for photosynthesis of higher investments in photosynthetic apparatus per leaf. However, both might not happen in reality, because fertilization experiments in TMCFs have shown that N addition does not always lead to increases in foliar N concentrations, or LAI (Tanner and others 1992; Fisher and others 2013). Furthermore, although the $V_{cmax}$–N relationship observed in this TMCF is significant, it contained notable between-species variance (van de Weg and others 2012). Nonetheless, irrespective of issues of N-limitation in TMCFs, the high absolute sensitivity of GPP to $V_{cmax}$ and $J_{max}$ emphasizes the importance of estimating these parameters accurately when modeling GPP.

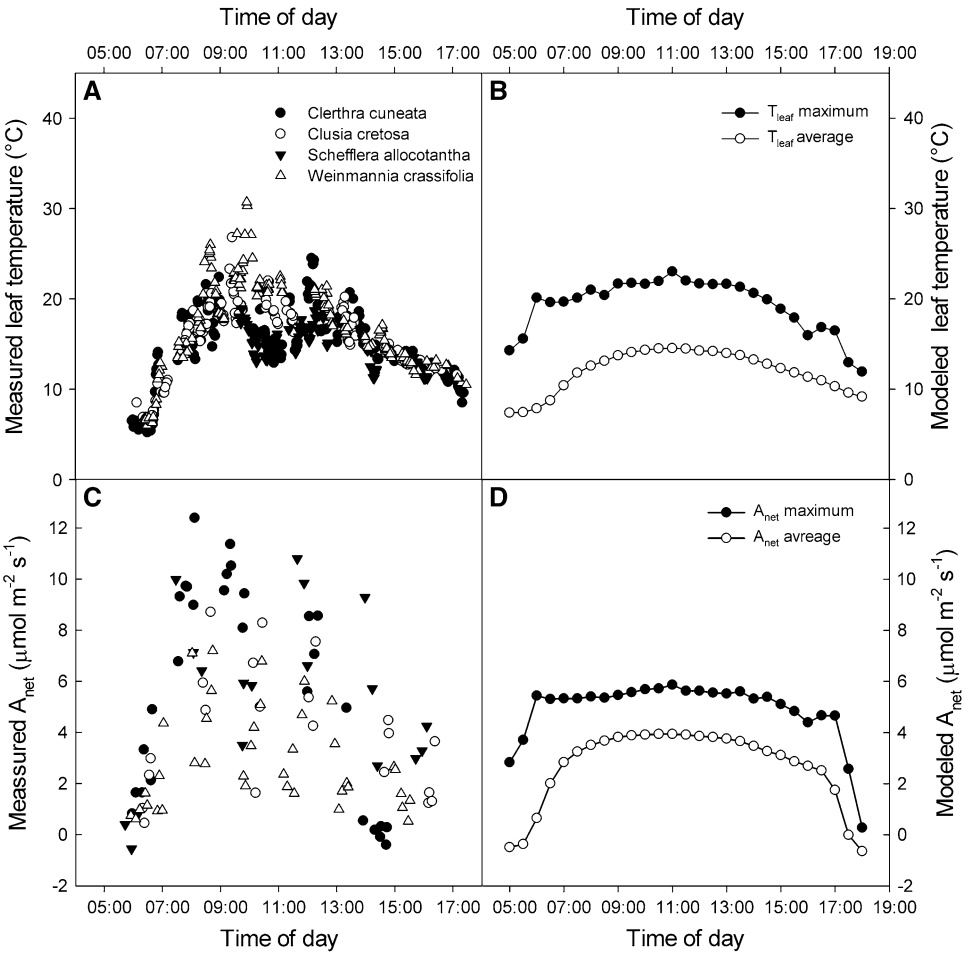


**Figure 4.** Diurnal measurements and modeled values of fully sunlit full grown leaves for $T_{leaf}$ (**A**, **B**) and $A_{net}$ (**C**, **D**). The measured values originate from the four abundant species measured in July and August 2008.

## Validation of the GPP Estimate

When we compare our GPP results with the modeled result from an altitudinal range of 450–1,050 m a.s.l. in the Luquillo mountains in Puerto Rico (Wang and others 2003), which was 60.3–24.1 Mg C $ha^{-1}$ $y^{-1}$, our GPP estimate is low. However, the model from Wang and others (2003) overestimated the high altitude GPP by 40% compared with field observations. This overestimation can be partially explained by the retrieval of their model parameters, as this was done remotely (that is, no site-derived parameters in the model). Furthermore, the average LAI values of their simulated transect were substantially overestimated (Wang and others 2003). In contrast, our results were based on detailed site-measured vegetation parameters and meteorological drivers. Overall, we find therefore it unlikely that our results represent a substantial underestimation compared to the results from Wang and others (2003).

Another TMCF GPP quantification, from the same 3,025 m a.s.l. TMCF in Peru, was based on the carbon expenditure of the forest [that is, the sum of all measured NPP and autotrophic respiration ($R_a$) terms] (Girardin and others 2013). At 25.9 ± 3.1 Mg C $ha^{-1}$ $y^{-1}$, this was 60% higher than our process-model based estimated of GPP, which is substantially larger than the intrinsic error for the SPA model of 10% (Fox and others 2009). Below we consider some factors that might explain this mismatch between the GPP estimates.

First, although SPA adequately simulated stomatal behavior, GPP could be underestimated if $A_{net}$ was underestimated. The two species *C. cuneata* and *S. allocotantha* had indeed much higher $A_{net}$ rates than the average modeled $A_{net}$ (Figure 4). However $A_{net}$ from *W. crassifolia* and *C. cretosa* was not dissimilar to the modeled values, and both these species together represent 46% of the trees in the plot, whereas *C. cuneata* and *S. allocotantha* together represent approximately 5%. If the unmeasured species in the plot (~50 species) have photosynthetic capacity similar to the latter species, rather than similar to *W. crassifolia* and *C. cretosa*, our simulated GPP might be underestimated. More specifically, a 20% higher plot average of $V_{cmax}$ and

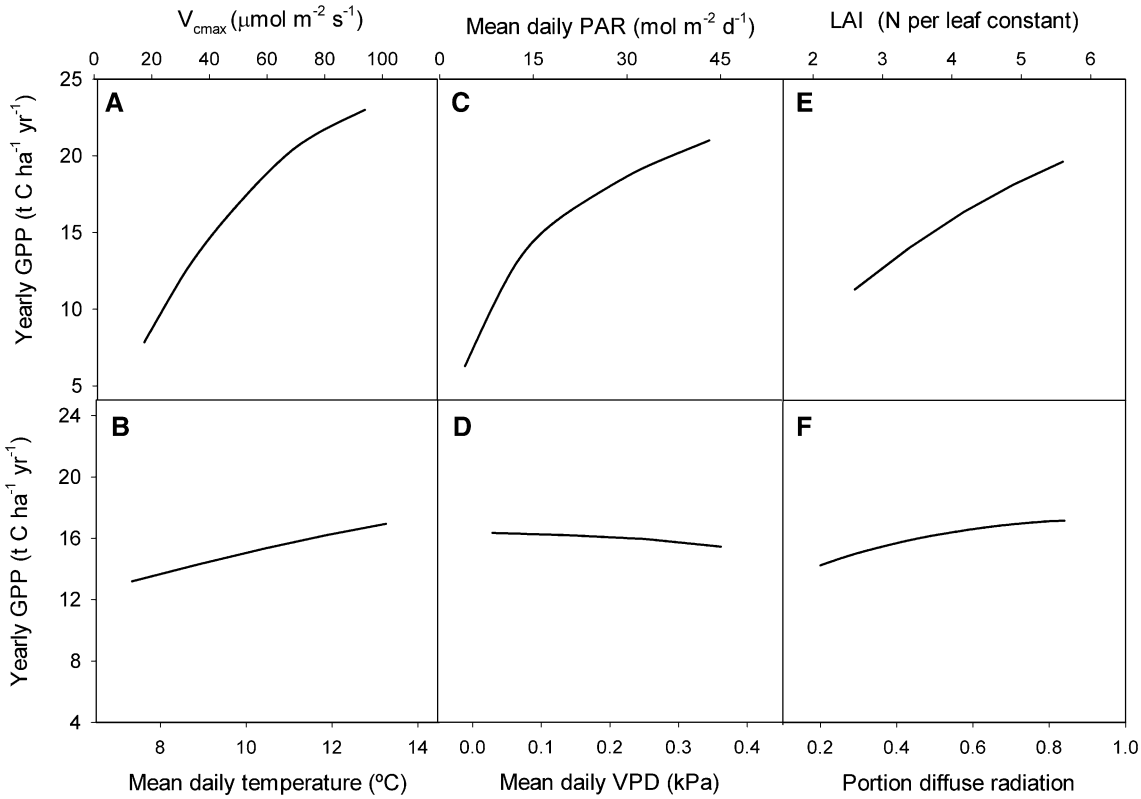


**Figure 5.** Results from the one-dimensional sensitivity analyses for six important factors over their observed range controlling annual TMCF GPP. Note that for panel **A**, both $V_{cmax}$ and $J_{max}$ were changed concurrently, whereas only $V_{cmax}$, and only the value of the top layer of the canopy is listed on the *X-axis*.

$J_{max}$, a plausible increase if the unmeasured species would behave like *C. cuneata* and *S. allocotantha*, would translate in an underestimation of GPP of 1.7 Mg C $ha^{-1}$ $y^{-1}$.

Another explanation for underestimated GPP comes from the modeling of $T_{leaf}$. Unfortunately, there are no published temperature–photosynthesis relationships for TMCF species. In the SPA model, this relationship is relatively shallow compared to that used, for example, by Sharkey and others (2007) (Supplementary Information III). Given that the photosynthetic parameters in the SPA model are based on measurements at $T_{leaf}$ approximately 20°C, and average simulated $T_{leaf}$ was around 15°C at mid-day (Figure 4B), it is unlikely that the temperature sensitivity of photosynthesis in SPA caused underestimations of modeled $V_{cmax}$ and $J_{max}$ (and hence $A_{net}$). A more plausible explanation comes from the underestimation of modeled $T_{leaf}$ compared with field-measured values (Figure 4A, B). The $T_{leaf}$ measurements between 8:00 and 17:00 were on average 3.25°C higher than the modeled values between those hours, and increasing modeled $T_{leaf}$ by 3.25°C would lead to 15.6% higher $V_{cmax}$ and $J_{max}$ values during the day time. For annual GPP values this implies a potential underestimation of about 1.3 Mg C $ha^{-1}$ $y^{-1}$ in our original model runs. Combined, the potential underestimation of photosynthetic parameter values ($V_{cmax}$ and $J_{max}$) and $T_{leaf}$ contributes up to one-third (~3.2 Mg C $ha^{-1}$ $y^{-1}$) of the 10 Mg C $ha^{-1}$ $y^{-1}$ discrepancy between the study from Girardin and others (2013) and this one.

The difference in GPP estimates from Girardin and others (2013) and this study can furthermore be explained by potential overestimates of the carbon expenditure ($R_a$ and NPP) in the former study, as this forms the basis for their GPP calculations. Girardin and others (2013) indicated that their values of $R_a$, and consequently GPP, could be overestimated due to uncertainties in scaling stem respiration ($R_{stem}$) from woody tissue surface area data. For example, Robertson and others (2010) report a stem area index (SAI) of 1.45 and a $R_{stem}$ of 0.62 μmol $m^{-2}$ $s^{-1}$ from a short campaign in the same site from which Girardin and others (2013) give an SAI of 2.03 and $R_{stem}$ of 1.1 mmol $m^{-2}$ $s^{-1}$.

Using the values from Robertson and others (2010), total $R_a$, and hence the GPP estimate, would be 5.6 Mg C $ha^{-1}$ $y^{-1}$ closer to our estimate. In addition, total $R_a$ could be overestimated by (Girardin and others 2013) because all day time respiration measures of $R_a$ were scaled to average daily temperature with a Q10 of 2.0 whereas Q10 values, in general, are higher in biomes with a lower average $T_{air}$ (Tjoelker and others 2001). For the research site, with an annual temperature of 12.5°C, application of the decline in Q10 with temperature proposed by Tjoelker and others (2001) would mean a Q10 of 2.65. If used, this would reduce $R_a$ and therefore GPP with 1.7 Mg C $ha^{-1}$ $y^{-1}$.

Quantifying uncertainty in the estimates from Girardin and others (2013) was beyond the aims of this study. Nonetheless, both possible underestimates of the modeled GPP in this study and possible overestimates in the summing of NPP and $R_a$ can explain the discrepancy of 10 Mg C $ha^{-1}$ $y^{-1}$ between two GPP estimates from the same research site. The large error terms in the component summation method have been acknowledged elsewhere and are currently difficult to constrain (for example, Malhi and others 2009; Girardin and others 2013). They offer a unique view into interpreting GPP, and we note that substantial reductions would be needed for them to account in isolation for the discrepancy between the two GPP estimates. Nonetheless, the use of site-, species-, and leaf-level data in the modeling exercise we present here is unprecedented for tropical montane forest physiology. Based on the GPP estimation of 16.2 Mg C $ha^{-1}$ $y^{-1}$ with potential underestimation of the model of 3.2 Mg C $ha^{-1}$ $y^{-1}$, it seems that the GPP of TMCFs at this altitude is indeed significantly smaller than lowland rainforest by 30–40%.

## Conclusions

This study presents a process-based simulated annual GPP of a TMCF, parameterized with field measurements of biochemical photosynthetic capacity ($V_{cmax}$ and $J_{max}$) and other physical vegetation parameters. The SPA model slightly underestimated daily transpiration rates when compared with in situ data, but simulated stomatal opening and closure correctly. In contrast, measurements of $A_{net}$ and $T_{leaf}$ indicate a potential underestimation of photosynthesis by the model. Overall, this modeling exercise confirms earlier hypotheses that (for tropical ecosystems) the long-observed low NPP of TMCFs is strongly influenced by lower GPP, which in turn is mostly explained by the characteristically lower $T_{air}$, PAR and LAI, though their relative importance may change with location and elevation. Furthermore, GPP decreases slightly in the dry season (with 17%), but not as a consequence of drought stress. Our analysis indicates that the GPP of our study TMCF at 3,025 m a.s.l. is substantially smaller than that of lowland rainforest, by 30–40% or more, and that this difference can be mostly attributed to the effect of lower temperatures. The uncertainties discussed in estimating GPP highlight the challenges that still exist in quantifying one of the most important fluxes in the terrestrial carbon cycle.

## Acknowledgments

This study is a product of the Andes Biodiversity and Ecosystems Research Group. This study was financed by a grant from the Andes-Amazon program of the Gordon and Betty Moore Foundation, with research grants from the UK Natural Environment Research Council, a Royal Geographical Society (with IBG) geographical fieldwork grant and a scholarship from the School of Geosciences from the University of Edinburgh. We also thank the Asociación para la Conservación de la Cuenca Amazónica (ACCA) for hosting us at the Wayqecha field station and INRENA for permitting us to explore the Peruvian tropical forest. We thank Rob St John for indispensible help with the sap flow system.

## References

Adamek M, Corre MD, Holscher D. 2009. Early effect of elevated nitrogen input on above-ground net primary production of a lower montane rain forest, Panama. J Trop Ecol 25:637–47.

Bruijnzeel LA, Veneklaas EJ. 1998. Climatic conditions and tropical, montane forest productivity: the fog has not lifted yet. Ecology 79:3–9.

Čermák J, Deml M, Penka M. 1973. A new method of sap flow rate determination in trees. Biol Plant 15:171–8.

Čermák J, Kucera J, Nadezhdina N. 2004. Sap flow measurements with some thermodynamic methods, flow integration within trees and scaling up from sample trees to entire forest stands. Trees Struct Funct 18:529–46.

Domingues TF, Berry JA, Martinelli LA, Ometto J, Ehleringer JR. 2005. Parameterization of canopy structure and leaf-level gas exchange for an eastern Amazonian tropical rain forest (Tapajos National Forest, Para, Brazil). Earth Interact 9(17): 1–23.

Farquhar GD, Caemmerer SV, Berry JA. 1980. A biochemical-model of photosynthetic $CO_2$ assimilation in leaves of C-3 species. Planta 149:78–90.

Fisher JB, Malhi Y, Torres IC, Metcalfe DB, van de Weg MJ, Meir P, Silva-Espejo JE, Huasco WH. 2013. Nutrient limitation in

rainforests and cloud forests along a 3,000-m elevation gradient in the Peruvian Andes. Oecologia 172(3):889–902.

Fisher JB, Malhi Y, Bonal D, Da Rocha HR, De AraÚJo AC, Gamo M, Goulden ML, Hirano T, Huete AR, Kondo H, Kumagai TO, Loescher HW, Miller S, Nobre AD, Nouvellon Y, Oberbauer SF, Panuthai S, Roupsard O, Saleska S, Tanaka K, Tanaka N, Tu KP, Von Randow C. 2009. The land–atmosphere water flux in the tropics. Glob Change Biol 15:2694–714.

Fisher RA, Williams M, da Costa AL, Malhi Y, da Costa RF, Almeida S, Meir P. 2007. The response of an eastern amazonian rain forest to drought stress: results and modelling analyses from a throughfall exclusion experiment. Glob Change Biol 13:2361–78.

Fisher RA, Williams M, de Lourdes Ruivo M, de Costa AL, Meir P. 2008. Evaluating climatic and soil water controls on evapotranspiration at two amazonian rainforest sites. Agric For Meteorol 148:850–61.

Fisher RA, Williams M, Do Vale RL, Da Costa AL, Meir P. 2006. Evidence from amazonian forests is consistent with isohydric control of leaf water potential. Plant Cell Environ 29:151–65.

Fox A, Williams M, Richardson AD, Cameron D, Gove JH, Quaife T, Ricciuto D, Reichstein M, Tomelleri E, Trudinger CM, Van Wijk MT. 2009. The REFLEX project: Comparing different algorithms and implementations for the inversion of a terrestrial ecosystem model against eddy covariance data. Agric For Meteorol 149(10):1597–615.

Girardin CAJ, Malhi Y, AragÃO LEOC, Mamani M, Huaraca Huasco W, Durand L, Feeley KJ, Rapp J, Silva-Espejo JE, Silman M, Salinas N, Whittaker RJ. 2010. Net primary productivity allocation and cycling of carbon along a tropical forest elevational transect in the Peruvian Andes. Glob Change Biol 16:3176–92.

Girardin CAJ et al. 2013. Productivity and carbon allocation in a tropical montane cloud forest in the Peruvian Andes. Plant Ecol Divers 7(1–2):55–69.

Grubb PJ, Whitmore TC. 1966. A comparison of montane and lowland rain forest in Ecuador. II. Climate and its effects on distribution and physiognomy of forests. J Ecol 54:303–33.

Hirata R, Saigusa N, Yamamoto S, Ohtani Y, Ide R, Asanuma J, Gamo M, Hirano T, Kondo H, Kosugi Y, Li S-G, Nakai Y, Takagi K, Tani M, Wang H. 2008. Spatial distribution of carbon balance in forest ecosystems across East Asia. Agric For Meteorol 148:761–75.

Hutyra LR, Munger JW, Hammond-Pyle E, Saleska SR, Restrepo-Coupe N, Daube BC, de Camargo PB, Wofsy SC. 2008. Resolving systematic errors in estimates of net ecosystem exchange of $CO_2$ and ecosystem respiration in a tropical forest biome. Agric For Meteorol 148:1266–79.

Kaimal JC, Finnigan JJ. 1994. Atmospheric boundary layer flows: their structure and measurement. Oxford: Oxford University Press.

Kitayama K, Aiba SI. 2002. Ecosystem structure and productivity of tropical rain forests along altitudinal gradients with contrasting soil phosphorus pools on Mount Kinabalu, Borneo. J Ecol 90:37–51.

Lemmon PE. 1956. A spherical densiometer for estimating forest overstory density. For Sci 2:314–20.

Letts MG, Mulligan M. 2005. The impact of light quality and leaf wetness on photosynthesis in north-west Andean tropical montane cloud forest. J Trop Ecol 21:549–57.

Malhi Y, Aragao L, Metcalfe DB, Paiva R, Quesada CA, Almeida S, Anderson L, Brando P, Chambers JQ, da Costa ACL, Hutyra LR, Oliveira P, Patino S, Pyle EH, Robertson AL, Teixeira LM. 2009. Comprehensive assessment of carbon productivity, allocation and storage in three Amazonian forests. Glob Change Biol 15:1255–74.

Marthews TR, Malhi Y, Girardin CAJ, Silva Espejo JE, Aragão LEOC, Metcalfe DB, Rapp JM, Mercado LM, Fisher RA, Galbraith DR, Fisher JB, Salinas-Revilla N, Friend AD, Restrepo-Coupe N, Williams RJ. 2012. Simulating forest productivity along a neotropical elevational transect: temperature variation and carbon use efficiency. Glob Change Biol 18:2882–98.

McMurtrie RE, Comins HN, Kirschbaum MUF, Wang YP. 1992. Modifying existing forest growth models to take account of effects of elevated $CO_2$. Aust J Bot 40:657–77.

Meir P, Kruijt B, Broadmeadow M, Kull O, Carswell F, Nobre A, Jarvis PG. 2002. Acclimation of photosynthetic capacity to irradiance in tree canopies in relation to leaf nitrogen concentration and leaf mass per unit area. Plant Cell Environ 25:343–57.

Miller SD, Goulden ML, Menton MC, da Rocha HR, de Freitas HC, e Silva Figueira AM, Dias de Sousa CA. 2004. Biometric and micrometeorologicla measurements of tropical forest carbon balance. Ecol Appl 14(Suppl. 4):114–26.

Moser G, Hertel D, Leuschner C. 2007. Altitudinal change in Lai and stand leaf biomass in tropical montane forests: a transect shady in Ecuador and a pan-tropical meta-analysis. Ecosystems 10:924–35.

Raich JW, Russell AE, Vitousek PM. 1997. Primary productivity and ecosystem development along an elevational gradient on Mauna Loa, Hawaii. Ecology 78:707–21.

Robertson AL, Malhi Y, Farfan-Amezquita F, Aragão LEOC, Silva Espejo JE, Robertson MA. 2010. Stem respiration in tropical forests along an elevation gradient in the Amazon and Andes. Glob Change Biol 16(12):3193–204.

Ryan MG, Binkley D, Fownes JH, Giardina CP, Senock RS. 2004. An experimental test of the causes of forest growth decline with stand age. Ecol. Monogr 74(3):393–414.

Santiago LS, Goldstein G, Meinzer FC, Fownes JH, Mueller-Dombois D. 2000. Transpiration and forest structure in relation to soil waterlogging in a Hawaiian montane cloud forest. Tree Physiol 20:673–81.

Saxton KE, Rawls WJ, Romberger JS, Papendick RI. 1986. Estimating generalized soil-water characteristics from texture. Soil Sci Soc Am J 50:1031–6.

Sharkey TD, Bernacchi CJ, Farquhar GD, Singsaas EL. 2007. Fitting photosynthetic carbon dioxide response curves for C-3 leaves. Plant Cell Environ 30:1035–40.

Tanner EVJ, Kapos V, Franco W. 1992. Nitrogen and phosphorus fertilization effects on Venezuelan montane forest trunk growth and litterfall. Ecology 73:78–86.

Tanner EVJ, Kapos V, Freskos S, Healey JR, Theobald AM. 1990. Nitrogen and phosphorus fertilization of Jamaican montane forest trees. J Trop Ecol 6:231–8.

Tanner EVJ, Vitousek PM, Cuevas E. 1998. Experimental investigation of nutrient limitation of forest growth on wet tropical mountains. Ecology 79:10–22.

Tjoelker MG, Oleksyn J, Reich PB. 2001. Modelling respiration of vegetation: evidence for a general temperature-dependent Q10. Glob Change Biol 7(2):223–30.

van de Weg MJ, Meir P, Grace J, Atkin OK. 2009. Altitudinal variation in leaf mass per unit area, leaf tissue density and foliar nitrogen and phosphorus content along an Amazon-Andes gradient in Peru. Plant Ecol Divers 2:243–54.

van de Weg MJ, Meir P, Grace J, Damian Ramos G. 2012. Photosynthetic parameters, dark respiration and leaf traits in the canopy of a Peruvian tropical montane cloud forest. Oecologia 168:23–34.

Vitousek P, Farrington H. 1997. Nutrient limitation and soil development: experimental test of a biogeochemical theory. Biogeochemistry 37:63–75.

Waide RB, Zimmerman JK, Scatena FN. 1998. Controls of primary productivity: lessons from the Luquillo Mountains in Puerto Rico. Ecology 79:31–7.

Wang HQ, Hall CAS, Scatena FN, Fetcher N, Wu W. 2003. Modeling the spatial and temporal variability in climate and primary productivity across the Luquillo Mountains, Puerto Rico. For Ecol Manage 179:69–94.

Williams M, Law BE, Anthoni PM, Unsworth MH. 2001a. Use of a simulation model and ecosystem flux data to examine carbon–water interactions in ponderosa pine. Tree Physiol 21(5):287–98.

Williams M, Malhi Y, Nobre AD, Rastetter EB, Grace J, Pereira MGP. 1998. Seasonal variation in net carbon exchange and evapotranspiration in a Brazilian rain forest: a modelling analysis. Plant Cell Environ 21:953–68.

Williams M, Rastetter EB, Fernandes DN, Goulden ML, Wofsy SC, Shaver GR, Melillo JM, Munger JW, Fan SM, Nadelhoffer KJ. 1996. Modelling the soil-plant-atmosphere continuum in a Quercus–Acer stand at Harvard Forest: the regulation of stomatal conductance by light, nitrogen and soil/plant hydraulic properties. Plant Cell Environ 19:911–27.

Williams M, Rastetter EB, Shaver GR, Hobbie JE, Carpino E, Kwiatkowski BL. 2001b. Primary production of an arctic watershed: an uncertainty analysis. Ecol Appl 11:1800–16.

Wright JK, Williams M, Starr G, McGee J, Mitchell RJ. 2013. Measured and modelled leaf and stand-scale productivity across a soil moisture gradient and a severe drought. Plant Cell Environ 36:467–83.

Wullschleger SD. 1993. Biochemical limitations to carbon assimilation in C3 plants: a retrospective analysis of the $A/C_i$ curves from 109 species. J Exp Bot 44:907–20.

Zimmermann M, Meir P, Bird MI, Malhi Y, Ccahuana AJQ. 2009. Climate dependence of heterotrophic soil respiration from a soil-translocation experiment along a 3000 m tropical forest altitudinal gradient. Eur J Soil Sci 60:895–906.

Zotz G, Tyree MT, Patino S, Carlton MR. 1998. Hydraulic architecture and water use of selected species from a lower montane forest in Panama. Trees Struct Funct 12:302–9.